

## Review

## Enzymatic biofuel cell: A potential power source for self-sustained smart textiles

Jingsheng Cai,<sup>1</sup> Fei Shen,<sup>2,\*</sup> Jianqing Zhao,<sup>2</sup> and Xinxin Xiao<sup>3,\*</sup>

## SUMMARY

**Self-sustained smart textiles require a miniaturized and flexible power source, while the state-of-the-art lithium-ion battery cannot be seamlessly integrated into smart textiles. Enzymatic biofuel cells (EBFC), utilizing physiological glucose or lactate as fuels to convert chemical energy into electricity, are a potential alternative power source. In comparison to other proposed energy harvesters relying on solar and biomechanical energy, EBFCs feature several key properties, including continuous power generation, biocompatible interfaces without using toxic elements, simple configuration without extra packaging, and biodegradability. There is an urgent need to introduce EBFCs to the researchers working on smart textiles, who typically are not expert on bioelectrochemistry. This minireview first introduces the working principle of EBFC and then summarizes its recent progress on fibers, yarns, and textiles. It's expected that this review can help to bridge the knowledge gap and provide the community of smart textiles with information on both the strengths and limitations of EBFCs.**

## INTRODUCTION

Nowadays, textiles not only satisfy traditional functions of body temperature maintenance and decoration, but fulfill health monitoring and therapeutic functions. These advanced textiles with enhanced functions are often referred to as smart textiles.<sup>1,2</sup> With the recent advances in materials science and electronic technology, smart textiles can serve as an excellent on-body platform for sensing body fluid metabolites,<sup>3,4</sup> arterial pulse monitoring,<sup>5</sup> body motion tracking,<sup>6</sup> thermotherapy<sup>7</sup> and drug delivery,<sup>8</sup> while retaining good wearing comfort. The rapid progress of smart textiles brings significant challenges for existing energy storage units, which are expected to be flexible, biocompatible, and undisrupted in providing power. These smart devices are normally powered by rechargeable lithium-ion batteries, which are, however, rigid, containing toxic chemicals. Therefore, there is an urgent need to explore flexible, bio-friendly, and sustainable energy systems for smart textiles. In comparison to energy storage based powers (i.e., batteries and supercapacitors) that require frequent charging, self-sustained powers that harvest electricity directly from the human body or the environment are promising, considering that the human body possesses adequate mechanical and chemical energy.

Enzymatic biofuel cells (EBFCs) are a type of electrochemical device converting chemical energy into electricity, featuring applications as wearable or implantable power sources. The first major advantage of EBFCs is the steady availability of biofuels. The chemical energy used by EBFCs can be from human body fluids, such as sweat, tears, blood, and saliva.<sup>9,10</sup> Abundant biofuels, including glucose and lactate, exist in the body fluids. These biofuels are renewable and contain energy up to 100 W,<sup>11–13</sup> satisfying the energy requirements of low-power consuming bioelectronics (200  $\mu$ W–1 W).<sup>14</sup> EBFCs utilizing biochemical fuels can provide relatively higher energy than other cells converting energy from body heat (4.8 W) or mechanical motions (67 W).<sup>15</sup> Second, EBFCs can continuously discharge as long as fuels are accessible and biocatalysts are active, while textile-based batteries need recharging after energy is exhausted. The third major advantage is the high biocompatibility of EBFCs. Enzymes are employed as biocatalysts to oxidize these biofuels for electricity generation in mild conditions. The good biocompatibility of EBFCs suggests the promise for implantable application. For example, an increase in cell viability (~150%) can be observed with EBFCs along with a relatively low inflammatory response.<sup>16</sup> Other advantages of EBFCs include simple cell configuration and small volume. EBFCs consist of the anode and cathode, even eliminating the requirement of device encapsulation, allowing high volumetric power density. Such a body-compliant energy harvesting device is thus very attractive for powering next-generation smart textiles for personalized healthcare.<sup>17–19</sup>

The marriage between EBFCs and fabric materials makes smart textiles possible. Fabric materials enjoy high flexibility, high stretchability, and wearability, making them favorable as interfaces between skin and electronics. Fabric materials are present in three different forms, arranged from bottom to top, namely fiber, yarn, and textile/fabric (Figure 1). Fiber, either naturally or artificially originated, is one-dimensional (1D) in diameter of tens to hundreds of microns. Yarn is made of fibers that are twisted or in a core-sheath configuration. Both fiber and yarn constitute the basis of two-dimensional or three-dimensional (2D/3D) textile/fabric, via a series of methods, such as weaving, knitting, and

<sup>1</sup>School of Materials Engineering, Changshu Institute of Technology, Changshu 215500, China

<sup>2</sup>Jiangsu Zoolnasm Technology CO., LTD, Suzhou 215000, China

<sup>3</sup>Department of Chemistry and Bioscience, Aalborg University, 9220 Aalborg, Denmark

\*Correspondence: feishen2019@outlook.com (F.S.), xixi@bio.aau.dk (X.X.)

<https://doi.org/10.1016/j.isci.2024.108998>



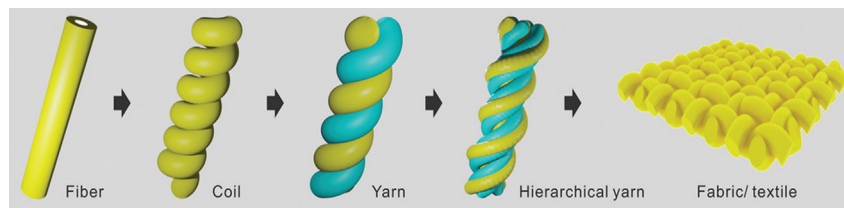


**Figure 1. The illustrative configurations of fibers, yarns and fabrics/textiles**

Reprinted with permission from Xiong et al.,<sup>20</sup> Copyright 2021, Wiley-VCH.

twisting. The word of textile/fabric could also be an umbrella term for all three forms. Challenges remain to seamlessly integrate EBFCs with fabric materials, which need to be converted into electrically conductive.

This minireview first introduces the working mechanism of EBFCs, and then summarizes the recent progress as energy sources for smart textiles, including 1D fiber-type and yarn-type EBFCs, and 2D/3D fabrics. Challenges and perspectives are presented at the end.

## FUNDAMENTALS OF ENZYMIC BIOFUEL CELLS

An EBFC is an electrochemical cell composed of two electrodes, similar to that in conventional fuel cells, except that enzymes are utilized as biocatalysts at one or both electrodes (Figure 2). Biofuels are oxidized by enzymes at the anode and donate electrons, which are transferred to the cathode through an external circuit. Blue copper enzymes or inorganic catalysts participate in the reduction of molecular dioxygen and then accept the electrons. Solid-state cathodes, such as Prussian blue (PB),  $\text{Ag}_2\text{O}/\text{Ag}$ , and  $\text{MnO}_2$ , that can accept electrons and are independent from oxygen reduction reaction (ORR), are also demonstrated.<sup>21</sup> According to the biofuels accessible by the implantable or wearable smart textiles, glucose oxidase (GOx)/dehydrogenase (GDH) and lactose oxidase (LOx) are commonly used at the anode. Regard to the cathodic enzyme, bilirubin oxidase (BOx) and laccase have been intensively studied due to the excellent ORR activity.<sup>22</sup> Besides, Pt/C catalysts used in traditional fuel cells are sometimes also employed at the cathode of EBFCs,<sup>23,24</sup> along with notable efforts devoted to developing noble metal free and non-enzymatic catalysts for ORR at physiological pH.<sup>25–27</sup>

Enzymes are macro biomolecules (typically several nm in size) and many of their redox sites are deeply embedded in an electrically inert protein matrix.<sup>28</sup> According to quantum mechanical electron transfer (ET) theory, the ET rate decreases exponentially with the electron tunneling distance,<sup>29,30</sup> and an upper threshold of 15–20 Å is confined for feasible ET.<sup>31–33</sup> Therefore, direct electron transfer (DET) between the redox centers of the enzymes and the electrode surfaces remains a challenge for most of the oxidoreductases.<sup>34</sup> DET feasible enzymes need to be properly oriented with their cofactor or ET relay centers as close to the electrode surface as possible.<sup>35–38</sup> BOx can undergo efficient DET for ORR with the assistance of three redox copper centers (types T1, T2, and T3).<sup>22</sup> T1 copper accepts electrons from the electron-donating substrates and shuttles them to the T2/T3 sites via intramolecular ET. As the T1 center is located at a short distance from the protein surface, rapid DET is achievable<sup>35</sup> (Figure 2). Alternatively, different artificial or biologically active charge carriers can be used for shuttling electrons between the enzyme cofactors and the electrodes, which refers to mediated electron transfer (MET). Synthetic redox compounds, including quinone compounds, transition-metal complexes, and others, have been widely investigated as mediators to exchange electrons with enzymes.<sup>39–42</sup> The formal redox potential of the mediator is crucial, which should be close to the potential of the cofactor of the enzyme to reduce potential loss of an EBFC, but with a reasonable difference permitting large current flow.<sup>43</sup>

Enzyme immobilization method is also crucial for achieving efficient ET process, considerable enzyme loading, reserving enzyme activity, and thus good EBFC performance. Commonly used immobilization methods include physical adsorption, polymer entrapment, covalent binding, and cross-linking, from weak to strong.<sup>28,44</sup> Physical adsorption is the mildest way for enzyme accommodation, benefiting for the reservation of enzyme structure and optimal orientation of enzymes. Thus, this method guarantees the maximum activity of enzymes but may lead to enzyme detachment during long-term operation. Entrapment leads to high enzyme loading but typically poor control over enzyme orientation.<sup>45–47</sup> Partial of the immobilized enzymes may not undergo DET if their active centers are located too far away from the electrode surfaces. Covalent binding and cross-linking provide strong enzyme attachment for long operation time at the cost of partial loss of catalytic activity and limited conformational transition.<sup>35</sup> There is no perfect construction strategy to meet all the requirements. The selection of immobilization approaches depends on several factors, such as the nature of the used enzyme, desired ET mechanism, and the practical application scenarios of EBFCs. An example is as for cellobiose dehydrogenase (CDH), which contains a FAD cofactor and a heme domain that are connected with each other through a flexible peptide linker. To permit rapid DET, the immobilization of CDH needs to enable high freedom of enzyme conformation change and physical adsorption is found to be the best method.<sup>38</sup>

Key parameters characterizing an EBFC are output current density, power density, open-circuit voltage (OCV), and operational stability.<sup>28</sup> However, the current state-of-the-art EBFCs register cell performances that are not yet competitive with those of conventional fuel cells.<sup>43</sup> The theoretical cell voltages of a glucose/ $\text{O}_2$  EBFC and a lactate/ $\text{O}_2$  EBFC at the standard condition are 1.18 (glucose is oxidized into gluconolactone) and 1 V (lactate is oxidized into pyruvate), respectively.<sup>43</sup> Most reported EBFCs that use sugars as biofuels generate an OCV less than 1 V, a maximum power density ( $P_{\text{max}}$ ) within  $1000 \mu\text{W cm}^{-2}$ , and an operational lifetime of hours and days.<sup>43,48</sup> Key solutions in improving EBFCs rely on: (i) the engineering of upgraded biocatalysts; (ii) the fine-tune of the interface between the enzyme and the electrode surface;

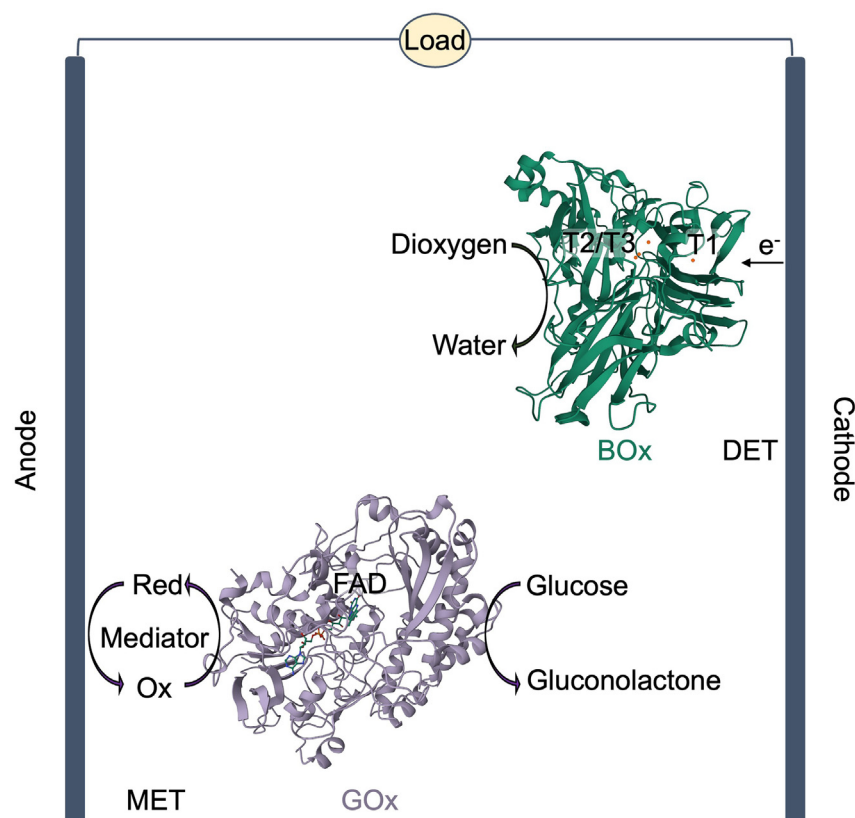


**Figure 2. Working mechanism of a glucose/O<sub>2</sub> EBFC consisting of a GOx (1CF3) bioanode and a BOx (2XLL) biocathode**  
Flavin adenine dinucleotide (FAD) is the cofactor of GOx.

(iii) the cell construction and nanomaterial introduction to the electrode; (iv) the enhanced supply of reactants to the bioelectrode. These points should be taken into account when designing a fabric based EBFC.

### FIBER-TYPE ENZYMATIC BIOFUEL CELLS

Fiber-type EBFCs have been extensively reported. They enjoy high flexibility and ease of miniaturization, showing great potential in implantable applications. Adjustable size and bending stiffness of fibers allow a mechanical match between the tissue and the device. Apart from size and flexibility, anti-fouling is another critical factor for *in vivo* application. Researchers usually coat a hydrophilic anti-fouling layer on the surface of fiber devices to prevent the nonspecific protein adsorption in a complex biological environment (Figure 3A).<sup>49,50</sup>

Commercially available fibers are firstly selected by researchers as electrode materials for enzyme immobilization and EBFC assembly because of the easy access. For example, commercial carbon fibers are attractive for enzyme immobilization and implantable applications, benefiting from their small dimensions and good biocompatibility. Mano et al. described a glucose/O<sub>2</sub> EBFC by crosslinking enzymes and redox polymers on carbon fibers (7- $\mu$ m diameter, 2-cm long).<sup>53</sup> A novel osmium complex modified redox polymer was employed as the mediator for accepting electrons from the FAD/FADH<sub>2</sub> cofactor in GOx with an onset potential as low as -0.1 V vs. Ag/AgCl for electrochemical oxidizing glucose. The cathode was composed of BOx and another osmium redox polymer. The miniaturized EBFC can operate continuously for one week and generated 0.9 J of electrical energy while passing a 1.7 C charge. Carbon fibers provide limited surfaces for enzyme accommodation, so carbon nanotubes (CNTs) are often used to improve the enzyme loading and electron transfer due to their high electrical conductivity and large surface area. To achieve direct power generation from biofuels in natural organisms, Yin et al. demonstrated a needle-type EBFC that integrated an Os-based polymer/CNT/GOx/Os-based polymer/CNT complex anode and a CNT/BOx/CNT cathode modified on carbon fibers, respectively.<sup>54</sup> When the anodic fiber was inserted into natural specimens with the help of a metallic hollow needle, the assembled EBFC could harvest high power in several fruits, including grape (55  $\mu$ W), kiwifruit (44  $\mu$ W), and apple (33  $\mu$ W). For *in vivo* mouse application, an anti-fouling polymer 2-methacryloyloxyethyl phosphorylcholine (MPC) layer was coated on both of the needle tip and the anode, generating a power of 16.3  $\mu$ W at 0.29 V from the blood glucose in heart tissue. Besides carbon fibers, other fiber materials have also been investigated as electrodes in EBFCs. Sim et al. reported a highly stretchable fiber-type EBFC by wrapping CNT/Enzyme/CNT multilayers on macromolecular rubber fibers, which can be reversibly stretched up to 100% in the tensile direction while outputting sustainable electrical power.<sup>55</sup> The unique rewinding structure, which trapped enzymes between CNT sheets, greatly enhanced the stability of the cell during

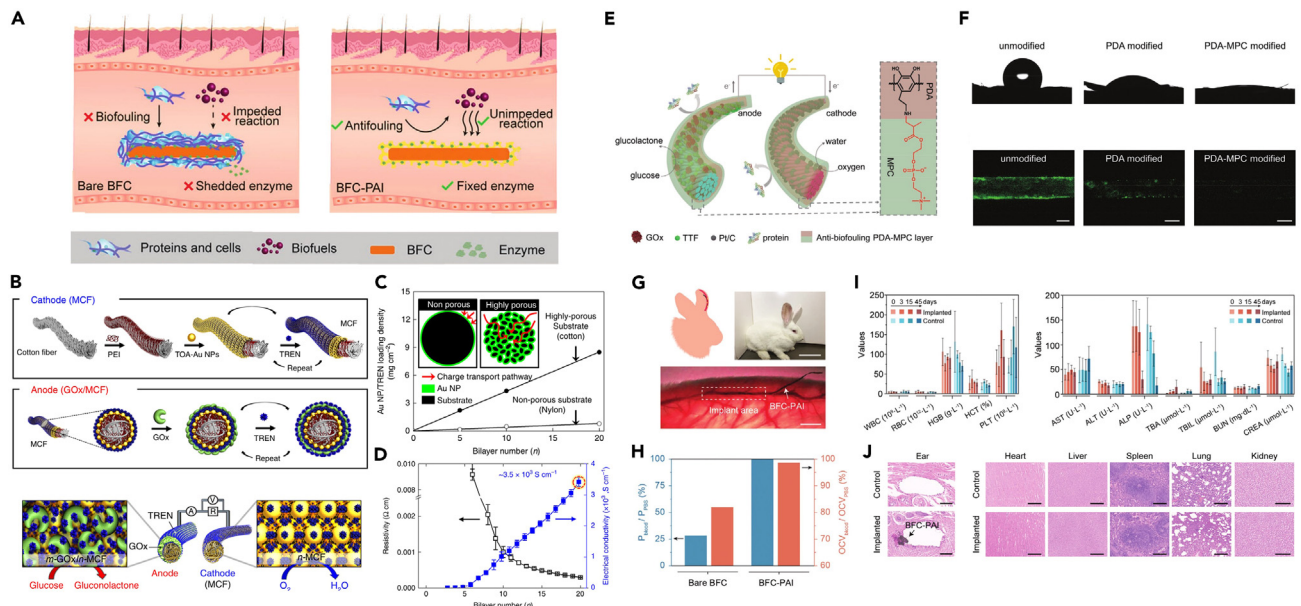


**Figure 3. Fiber-type enzymatic biofuel cells and their practical applications**

- (A) Schematic illustration of an EBFC operated *in vivo* with/without an anti-fouling protecting layer. Reprinted with permission from Wang et al.<sup>49</sup> Copyright 2021, Wiley-VCH.
- (B) Illustration of the preparation of an MCF-based cathode and GOx/MFC-based anode, and their combination as an EBFC.
- (C) Charge transport pathway differences of porous cotton fibers and nonporous nylon fibers coating with same number of AuNPs bilayers.
- (D) Resistivity and electrical conductivity of MCFs as a function of bilayer numbers. Reprinted with permission from Kwon et al.<sup>51</sup> Copyright 2018, Nature Publishing Group.
- (E) Schematic illustration of a fiber EBFC with PDA-MPC anti-biofouling layers.
- (F) The water contact angles and confocal fluorescence microscopy images of FITC-BSA treated of unmodified, PDA modified and PDA-MPC modified CNT electrodes (Scale bar, 30  $\mu\text{m}$ ). Reprinted with permission from Guo et al.<sup>52</sup> Copyright 2022, Wiley-VCH.
- (G) Implantation application of BFC-PAI in rabbit.
- (H) Comparison of the changes of power density and OCV of bare BFC and BFC-PAI operated from PBS solution to blood.
- (I) The changes of blood indexes for 45 days implantation, including white blood cell (WBC), red blood cell (RBC), hemoglobin (HGB), platelet (PLT), hematocrit (HCT), aspartate transaminase (AST), alaninetransaminase (ALT), alkaline phosphatase (ALP), total bile acid (TBA), total bilirubin (TBIL), blood urea nitrogen (BUN), and creatinine (CREA).
- (J) Representative histological analysis, including blood vessel, heart, liver, spleen, lung, and kidney of rabbit after implantation for 45 days and non-implanted controls. Reprinted with permission from Wang et al.<sup>49</sup> Copyright 2021, Wiley-VCH.

the fiber deformation. The EBFC with a diameter of  $\sim 380 \mu\text{m}$  operated well in human serum ( $36.6 \mu\text{W cm}^{-2}$ ). As shown in Figure 3B, cotton fibers with highly porous surfaces and intrinsic flexibility were also selected as electrode materials through uniformly and densely coating AuNPs onto the cellulosic fibers.<sup>51</sup> The resulting metallic cotton fibers (MCFs) displayed electrical properties (a high conductivity of  $\sim 3.5 \times 10^3 \text{ S cm}^{-1}$  and a low resistivity of  $\sim 1.2 \times 10^{-4} \Omega \text{ cm}$ ) close to those of bulk Au wire (Figures 3C and 3D). GOx was electrostatically adsorbed onto the MCFs with the help of an amine-functional small-molecule linker, tris-(2-aminoethyl) amine. Combined with an MCF based cathode undergoing ORR, the hybrid EBFC provided a remarkable power density of  $3.7 \text{ mWcm}^{-2}$  without the aid of redox mediators.

Apart from utilizing commercial fibers, researchers keep working on developing novel fiber materials to meet the requirements for implantable application. Peng's group reported a type of multi-walled carbon nanotubes (MWCNTs) assembled fiber bundles inspired by the hierarchical structure of muscles, which could be adapted to the range of bending stiffnesses for most tissues, such as muscles and blood vessels.<sup>56</sup> The flexible fiber can be precisely injected into the target tissues and maintains a robust and stable device-tissue interface *in vivo*, addressing the challenges for random-target implantation and long-term monitoring. Moreover, the large surface areas of CNT fiber electrodes enable high loading of enzymes and mediators. GOx and Pt/C were selected as catalysts immobilized on the fiber electrodes to achieve a bioanode and a biocathode, respectively (Figure 3E).<sup>52</sup> After *in situ* polymerization of a hydrophilic zwitterionic polydopamine-2-methacryloyloxyethyl phosphorylcholine (PDA-MPC) layer, the fiber EBFC was successfully implanted into a mouse brain for one month and displayed high resistance to nonspecific protein adsorption. The excellent anti-biofouling performance of fiber EBFC was attributed to the hydrophilicity of the PDA-MPC layer, which can be characterized by the water contact angle and fluorescein isothiocyanate-tagged BSA (FITC-BSA) binding analysis. The PDA-MPC modified fiber electrode showed the smallest water contact angle ( $13^\circ$ ) and lowest sign of massive protein adsorption compared to those of the PDA modified and bare electrodes (Figure 3F). As a result, the fiber EBFC maintained a long-term stability *in vivo*, holding great promise as an energy-harvesting device in complex biological fluids.

Traditional antifouling layer such as polyvinyl alcohol (PVA) shows similar antifouling performance to EBFC because the abundant hydroxyl groups on the polymer backbone can interact with water molecules to form a hydration shell to resist the adsorption/adhesion of cells and proteins,<sup>57–59</sup> but leads to poor immobilization ability to enzymes. Combining PVA with cationic polymer poly(vinyl alcohol)-N-methyl-4(4'-formylstyryl) pyridiniummethosulfateacetal (PVA–SbQ), polymer matrix with 3D porous structure was formed, which not only resisted the biofouling from body fluid, but also promoted the immobilization of enzymes via electrostatic attraction between negatively charged amino acid chains of enzymes and positively charged styrylpyridinium side chains in PVA–SbQ.<sup>49</sup> A porous antifouling interface (PAI) was therefore formed on the surface of the EBFC to promote its electrochemical performance and biocompatibility in body fluids. After implanted into the ear vein of a rabbit for 45 days, the PAI coated EBFC can maintain almost 100% performance (a maximal output power of  $76.6 \text{ mW cm}^{-3}$ ), and the blood index and histological analysis showed no significant differences between implanted samples and controls (Figures 3G and 3H). To achieve higher power output, polyaniline (PANI) electrodeposited on CNT fibers was fabricated as charge storing components to combine with the EBFCs. The resulting hybrid fiber cell was successfully implanted into the subcutaneous tissue of a rat, and can realize effective electrical stimulation to the sciatic nerve.<sup>60</sup>

### YARN-TYPE ENZYMATIC BIOFUEL CELLS

Yarns as an intermediate type of fabric between fibers and textiles, can be easily fabricated from fibers or be woven to textiles.<sup>61</sup> Yarns have the similar dimension as fibers, thus can be also applied in implantation. Kim's group explored a series of work toward CNT yarn based EBFCs.<sup>62,63</sup> First, poly(3,4-ethylenedioxythiophene) (PEDOT) was employed to coat on CNTs. The hydrophilic PEDOT coating not only enabled high loading of enzymes and redox mediators, but improved the tolerance to antagonistic chemical species (such as urate, chloride ion, and ascorbic acid) in human body fluids ascribed to the cation-exchange nature of the polymer.<sup>64,65</sup> Then, the PEDOT-coated MWCNT sheets were used as host materials for enzyme and mediator immobilization to fabricate bistructured yarn electrodes for both anode and cathode through a twisting method.<sup>62</sup> The corridor structure between scrolled PEDOT/MWNT sheets in the bistructured yarn provided a continuous internal pathway for rapid fuel diffusion and ion transport from surface to center, as well as sufficient porosity through scroll layers for cross-layer transport. Although redox mediators were used for electron shuttle,  $\text{O}_2$  in electrolyte competed with mediators in the GOx anode, inducing current density decrease in oxygen-saturated electrolyte. On the other hand, cathodic performance improved with the increase in oxygen concentration. The assembled yarn EBFC provided an OCV of 0.70 V, and a  $P_{\text{max}}$  of  $2.18 \text{ mW cm}^{-2}$ . In addition, the influence of biofluid flow rate was explicitly investigated as it is important for animal/human implantations.<sup>63</sup> Power densities grow by increasing the stirring, which was relevant with the effect of varies blood flow rates (for example,  $0.5 \text{ L min}^{-1}$  near liver,  $0.55 \text{ L min}^{-1}$  near kidney, and  $5.25 \text{ L min}^{-1}$  near heart of human body.<sup>66</sup> The yarn EBFC was surgically implanted into the abdominal cavity of a mouse after coating a Nafion layer.<sup>67</sup> A slight acute immune response was observed on the first day, which was attenuated after 7 days, indicating the good *in vivo* biocompatibility of the yarn EBFC. To avoid toxicity associated with the possible leakage of metal-based redox mediators, a mediator-free CNT based yarn EBFC was fabricated.<sup>68</sup> The weight percentage of PEDOT on the MWCNT electrode was crucial for modulating the surface structure for enzyme loading. A relatively low concentration of PEDOT (2 wt. %) was found to be optimal. When the PEDOT-MWCNT sheet was separated from the enzyme solution and left to dry, surface tension induced self-assembly of an MWCNT yarn. The electrons generated from the enzymatic reaction can be easily transferred through the yarn electrode because of the shrinkage between enzymes and MWCNTs during the water evaporation. Moreover, this electrode structure can effectively entrap the enzymes by the hydrophobic interactions between MWCNTs, therefore enhancing the stability of the EBFC. A  $P_{\text{max}}$  of  $236 \mu\text{W cm}^{-2}$  was achieved by the EBFC, which is however much lower than the mediated yarn EBFC.

### FABRIC-TYPE ENZYMATIC BIOFUEL CELLS

The rapid growing of wearable electronics has stimulated the development of on-body energy-harvesting strategies. Due to the good biocompatibility and utilization of fuels from non-invasive biofluids, fabric-type EBFCs become one of the most promising power sources for next generation smart textiles. A series of “scavenge-sense-display” devices have been proposed, which can “scavenge” biochemical energy from the wearer's perspiration, “sense” the biomarker level, and simultaneously “display” to the readout. For instance, researchers utilized tailored stretch-enduring inks and judicious design patterns to screen-print bioelectronic devices onto stretchable textile substrates, such as headbands, straps and socks (Figures 4A and 4C).<sup>69</sup> The stretchable EBFC array was designed by first screen printing a 75 mm thick layer of Ecoflex on a stretchable textile, followed by a same thickness layer of polyurethane (PU). Afterward, a sequence of stretchable Ag/AgCl and CNT inks were printed for enzyme immobilization and conductivity improvement. The bioanode was functionalized with a single enzyme (i.e., GOx or LOx) and 1,4-naphthoquinone (NQ) as a redox mediator for the biocatalytic oxidation of biofuels (Figure 4B(a)). An  $\text{Ag}_2\text{O}/\text{Ag}$  redox couple electrode was selected as a consumed type cathode, which does not rely on the ORR and can thus operate under anaerobic conditions (Figure 4B(b)). The obtained EBFC guaranteed mechanical resilience, accommodating stress such as multiaxial stretching, bending, wrinkling, stretching. As a result, the stretchable EBFC can operate on human-body sweat to harvest energy and provide a self-powered response (Figure 4D). The  $P_{\text{max}}$  achieved from the textile-based glucose EBFC was  $160 \text{ mW cm}^{-2}$  with an OCV of 0.44 V (Figure 4E). To illustrate the fully autonomous sensing system in the mechanically compliant wearable platform, short circuit current responses, generated by the sensor itself, were recorded when no voltage was applied. The wearable self-powered sensor displayed a real-time signal of lactate concentrations with a good linearity up to 20 mM lactate and a limit of detection of 0.3 mM (Figure 4F). As the variable levels of sweat and lactate limit a constant power output of the EBFC, a supercapacitor (SC) component printed on the opposite side of the textile substrate was integrated together with the previous LOx/ $\text{Ag}_2\text{O}$  EBFC.<sup>70</sup>  $\text{MnO}_2/\text{CNT}$  composites served as active materials for energy storage due to their



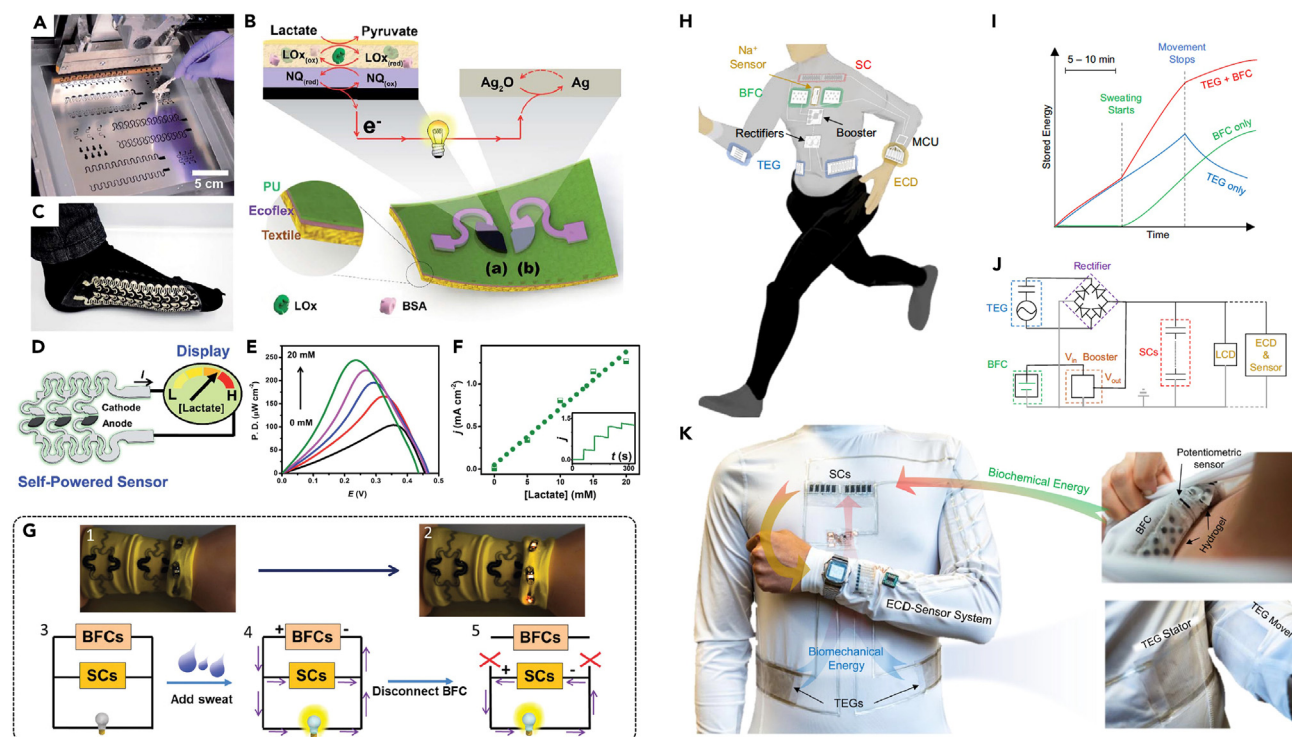


**Figure 4. Fabric-type enzymatic biofuel cells and their practical applications**

- (A) Photograph of the designed stencil used for printing stretchable devices and the screen-printing process.
- (B) Schematic illustration of the stretchable lactate EBFC and the redox reactions that occur on the anode (a) and cathode (b), respectively.
- (C) A self-powered sensor printed on a sock worn by a volunteer.
- (D) Schematic illustration of the integrated “scavenge-sense-display” system.
- (E) Power curves of the stretchable nylon-spandex textile-based lactate EBFC at varying lactate concentrations (0, 5, 10, 15, and 20 mM).
- (F) The self-generated current response obtained from the stretchable lactate EBFC, with no applied potential. Reprinted with permission from Jeerapan et al.<sup>69</sup> Copyright 2016, The Royal Society of Chemistry.
- (G) Demonstration of the hybrid SC-EBFC device. (1 and 2) Photographs showing the application of three SCs charged by five EBFCs to light LEDs using the following procedure: (3) without lactate, no power; (4) with lactate, LEDs were turned on; (5) upon disconnecting EBFCs and SCs, LEDs could still be turned on. Reprinted with permission from Lv et al.,<sup>70</sup> Copyright 2018, The Royal Society of Chemistry.
- (H) Systematical diagram of the microgrid system, consisting of the TEG, EBFC, SC modules and wearable applications.
- (I) Graphic illustration of the synergistic effect of integrating the complementary EBFC and TEG energy harvesters.
- (J) Multi-module e-textile microgrid for powering an LCD or an ECD-sensor system.
- (K) Photograph of the integration of a microgrid system on a practical shirt worn on-body. Reprinted with permission from L. Yin et al.<sup>71</sup> Copyright 2021, Nature Publishing Group.

high areal capacitance and good cycling stability. As shown in Figure 4G, feeding 10 mM lactate fuel solution on the EBFCs turned the LED “on” and charged the SCs simultaneously. Disconnected from the EBFCs, the SCs can still light the LEDs. The textile-based hybrid devices allowed stable power output even with the fluctuated sweat amount and thus promoted the development of self-powered wearable electronics. In addition, the same group explored to unite two different type energy harvesters (EBFCs and triboelectric generators (TEGs)) and energy storage modules into a wearable e-textile microgrid system to maximize the overall efficiency and performance for desired applications (Figure 4H).<sup>71</sup> As EBFCs and TEGs adopt distinct energy harvesting mechanisms, they perform complementary collection of energy from human motion for powering the SC modules, which integrate low-current, high voltage inputs from the TEG modules firstly and high-current, low-voltage inputs from the EBFC modules after sweating during human movements (Figure 4I). With optimized pairing of components, the multi-module e-textile microgrid was able to quickly boot selected applications such as a microwatt-rated liquid crystal display (LCD) wristwatch or a milliwatt-rated sensor-electro-chromic display (ECD) system (Figure 4J). The microgrid system was successfully printed on a shirt to scavenge energy from human motion, demonstrated an attractive example for future multi-functional smart textiles that are autonomous, reliable, synergistic, sustainable, and energy-efficient (Figure 4K).

In addition to the screen-printing method, researchers developed other methods to fabricate textile EBFCs. Similar to the screen-printing method but using machines, Kai et al. demonstrated a LOx/BOx EBFC by directly painting conductive CNT suspension on textile meshes.<sup>72</sup> Enzymes and mediators were then modified onto the CNT-coated fabric in a dropwise manner. As native LOx has a low Michaelis constant of

**Table 1. The performance comparison and practical application of fiber-type, yarn-type and fabric-type EBFCs**

	Anode	Cathode	Maximum power (density)	Stability	Practical application	Reference
Fiber-type EBFCs	GOx and Os-polymer coated on carbon fibers	BOx and Os-polymer coated on carbon fibers	4.3 $\mu\text{W mm}^{-2}$	64% retained after one week continuously operation	/	Mano et al. <sup>53</sup>
	GOx modified on metallic cotton fiber	Metallic cotton fiber	3.7 $\text{mW cm}^{-2}$	~62% maintained after continuous operations for 35 days	/	Kwon et al. <sup>51</sup>
	GOx and Os-based polymer coated on CNT wrapped rubber fibers	BOx and Os-based polymer coated on CNT wrapped rubber fibers	39.5 $\text{mW cm}^{-2}$	~86% retained after 10 h of continuous operation	Tested in human serum <i>in vitro</i>	Sim et al. <sup>55</sup>
	Os-based polymer/CNT/GOx/Os-based polymer/CNT complex modified on carbon fibers	CNT/BOx/CNT cathode modified on carbon fibers	55 $\mu\text{W}$	86% remained after continuous operation for 7.0 h	Tested in grape, kiwifruit, apple, and mouse	Yin et al. <sup>54</sup>
	GDH based PAI precursor solution dipped onto CNT fibers	BOx based PAI precursor dipped onto CNT fibers	76.6 $\text{mW cm}^{-3}$	~90% maintained after operating 2 h	Tested in the ear vein of a rabbit	Wang et al. <sup>49</sup>
	GOx and PDA-MPC layer immobilized on CNT fibers	Pt/C PDA-MPC layer immobilized on CNT fibers	~4.4 $\mu\text{W cm}^{-2}$	57% remained after implanted for over a month	Power generation in a mouse brain	Guo et al. <sup>52</sup>
Yarn-type EBFCs	GOx and Os-based polymer linked on twisted PEDOT/MWCNT yarns	BOx and Os-based polymer linked on twisted PEDOT/MWCNT yarns	2.18 $\text{mW cm}^{-2}$	83% remained after 24 h continuous operation	Tested in human serum <i>in vitro</i> and weaved into a textile	Kwon et al. <sup>62</sup>
	GOx adsorbed on PEDOT/MWCNT yarns	BOx adsorbed on PEDOT/MWCNT yarns	236 $\mu\text{W cm}^{-2}$	84% retained after 20 days' continuous operation	/	Kwon et al. <sup>68</sup>
	GOx and Os-based polymer modified on PEDOT/MWCNT yarns	BOx and Os-based polymer modified on PEDOT/MWCNT yarns	0.73 $\text{mW cm}^{-2}$	81% retained after 7 days' continuous operation	Tested in the abdominal cavity of mice	Lee et al. <sup>67</sup>
Fabric-type EBFCs	GOx or LOx/NQ/OH-CNTs drop casted on BFC arrays screen printed stretchable textiles	Stretchable Ag <sub>2</sub> O/Ag electrode	250 $\mu\text{W cm}^{-2}$	No significant variation in the shape and power density after 100% stretching up to 150 iterations	Powered LEDs or worked as self-powered lactate sensors after screen printed on socks	Jeerapan et al. <sup>69</sup>
	LOx/NQ/CNTs drop casted on BFC arrays screen printed stretchable textiles	BOx/CNT/protoporphyrin IX drop casted on BFC arrays screen printed stretchable textiles	21.5 $\mu\text{W}$	No change in power after bending 1000 times; ~88% after 7 days' storage	Powered an liquid crystal display wristwatch or a sweat ECD after integrated into e-textile microgrids	Yin et al. <sup>71</sup>
	LOx/tetrathiafulvalene/CNT painted on stretchable fabric	BOx/CNT painted on carbon fiber fabric	/	/	Self-powered lactate sensors after fabricated on textile meshes	Kai et al. <sup>72</sup>
	GDH/methylene green/CNT dropped onto carbon fibers	BOx/CNT dropped onto carbon fibers	216 $\mu\text{W cm}^{-2}$	/	Powered an LED device after woven on a textile cloth	Yin et al. <sup>74</sup>

1.0 mM,<sup>10</sup> polyurethane was coated on the anode surface to limit the permeability to lactate, modulate its concentration profile, and increase the linear range. The amperometric response of the lactate sensor showed a wide concentration range (5 to  $\geq 20$  mM) on the artificial perspiration device. In addition, graphene/CNT composites could grow on a nickel fiber in the textile through a two-step chemical vapor deposition (CVD) method.<sup>73</sup> CNT arrays were aligned on graphene layers, offering channels for effective charge transfer. The nickel substrate was then etched by a solution method to achieve lightweight and flexible electrodes. GOx and BOx were immobilized onto the graphene/CNTs electrodes as the anode and cathode, respectively. Along with using a polyacrylamide hydrogel electrolyte containing glucose, the assembled EBFC was able to tolerate bending angles from 0° to 180° and maintained 93.5% of its original power density under a tensile strain as high as 60%. Besides, previously described flexible fiber-type and yarn-type EBFCs can be woven on the cloth to fabricate autonomous energy harvesting garments.<sup>62,74</sup>

## CONCLUSION AND PERSPECTIVES

This review summarizes the recent advances of EBFCs fabricated on different forms of fabrics: fiber, yarn, and textile. The different dimensions of material structures affect the performance of the corresponding EBFCs. For fibers and yarns, large surface areas are exposed for enzyme immobilization and enzyme substrate, while only the outmost surfaces are typically utilized for textiles. As a result, fiber and yarn-type EBFCs usually display relatively higher energy densities than textile-type cells (Table 1). Benefiting from the high flexibility and adjustable size, fiber and yarn types show great potential as implantable power supply units, especially after coating with hydrophilic anti-fouling layers. Large dimensional yarn and fabric types can be facilely integrated into commercial garments for powering wearable electronics. As demonstrated in the literature, EBFCs hold the promise as the power source for next generation smart textiles due to their excellent biocompatibility, adequate biofuel available and ease-of-miniaturization. However, it's noteworthy that the development of EBFCs in smart textiles is still at the very early stage, as most reports merely focus on the construction and performance test of fabric type EBFCs. There are few studies describing prototypes of integrated smart textile systems consisting of powering, sensing, and communicating units, that are powered by EBFCs. It's thus crucial to bring interdisciplinary efforts of the smart textile community to push the frontier of the research. A highly integrated platform is only possible with miniaturized and low-energy consuming microelectronics. Furthermore, the standard evaluation protocols of smart textiles are still lacked, such as their specific current and power, device flexibility, and wearing stability. Clear criteria, which guide researchers to improve their work, are highly desirable.

For *in vivo* application, EBFCs are immersed in a complex biological environment with various flowing biomolecules and redox species, and thus easily induced function failure due to a range of reasons, such as biofouling, enzyme deactivation, inflammatory reaction, and insufficient biofuel supply. Adequate implantation site selection in living beings is of great importance to allow sufficient fuel supply, efficient removal of catabolites to avoid local toxicity.<sup>13</sup> The anti-fouling property on the surface of EBFCs is another critical factor for minimizing nonspecific protein adsorption and maintaining stable long-term operation. Biodegradation is appealing, but there is no report yet of a fully biodegradable fiber EBFC.

For the fabric-type EBFC itself, the performance is still constrained. In practice, single EBFCs suffer from low power density, limited output voltage, and poor operational lifetime deriving from the intrinsic nature of the enzymes. Enzyme engineering offers a promising approach to overcome such an intrinsic limitation. Massive efforts have been devoted into the developing novel electrode materials to accommodating enzyme for improved electron transfer, enzyme loading, and restoring original activity. This in turn will inspire the design of new fabric materials for enhanced EBFC performance.

In parallel, given the current performance of EBFCs, integration of EBFCs with other energy-harvesting devices (such as thermoelectric, piezoelectric, and triboelectric generators) and energy-storage systems (such as batteries and supercapacitors) could provide high flexibility for sustainably powering smart textiles. Meanwhile, the series or parallel connection of multiple EBFCs is feasible for wearable applications to enhance the output voltage or power, respectively. However, it's not feasible to improve the output voltage by series connection of several EBFCs for implantable applications due to the ionic short-circuiting.

## ACKNOWLEDGMENTS

J.C. acknowledges a start-up research grant for a professor at Changshu Institute of Technology. X.X. acknowledges a Villum Experiment (grant No. 35844) and a Novo Nordisk Foundation Start Package grant (0081331).

## DECLARATION OF INTERESTS

The authors declare no competing interests.

## REFERENCES

- Libanori, A., Chen, G., Zhao, X., Zhou, Y., and Chen, J. (2022). Smart textiles for personalized healthcare. *Nat. Electron.* 5, 142–156. <https://doi.org/10.1038/s41928-022-00723-z>.
- Zhang, Y., Wang, H., Lu, H., Li, S., and Zhang, Y. (2021). Electronic fibers and textiles: Recent progress and perspective. *iScience* 24, 102716. <https://doi.org/10.1016/j.jisci.2021.101616>.
- He, W., Wang, C., Wang, H., Jian, M., Lu, W., Liang, X., Zhang, X., Yang, F., and Zhang, Y. (2019). Integrated textile sensor patch for real-time and multiplex sweat analysis. *Sci. Adv.* 5, eaax0649. <https://doi.org/10.1126/sciadv.aax0649>.
- Wang, L., Wang, L., Zhang, Y., Pan, J., Li, S., Sun, X., Zhang, B., and Peng, H. (2018). Weaving sensing fibers into electrochemical fabric for real-time health monitoring. *Adv. Funct. Mater.* 28, 1804456. <https://doi.org/10.1002/adfm.201804456>.
- Meng, K., Zhao, S., Zhou, Y., Wu, Y., Zhang, S., He, Q., Wang, X., Zhou, Z., Fan, W., Tan, X.,



- Yang, J., and Chen, J. (2020). A wireless textile-based sensor system for self-powered personalized health care. *Matter* 2, 896–907. <https://doi.org/10.1016/J.MATT.2019.12.025>.
6. Luo, Y., Li, Y., Sharma, P., Shou, W., Wu, K., Foshey, M., Li, B., Palacios, T., Torralba, A., and Matusik, W. (2021). Learning human–environment interactions using conformal tactile textiles. *Nat. Electron.* 4, 193–201. <https://doi.org/10.1038/s41928-021-00558-0>.
7. Zhao, X., Wang, L.Y., Tang, C.Y., Zha, X.J., Liu, Y., Su, B.H., Ke, K., Bao, R.Y., Yang, M.B., and Yang, W. (2020). Smart  $\text{Ti}_3\text{C}_2\text{T}_x$  MXene fabric with fast humidity response and joule heating for healthcare and medical therapy applications. *ACS Nano* 14, 8793–8805. <https://doi.org/10.1021/ACS.NANO.0C03391>.
8. Amjadi, M., Sheykhansari, S., Nelson, B.J., and Sitti, M. (2018). Recent advances in wearable transdermal delivery systems. *Adv. Mater.* 30, 1704530. <https://doi.org/10.1002/ADMA.201704530>.
9. ul Haque, S., Yasir, M., and Cosnier, S. (2022). Recent advancements in the field of flexible/wearable enzyme fuel cells. *Biosens. Bioelectron.* 214, 114545. <https://doi.org/10.1016/j.bios.2022.114545>.
10. Xiao, X., Conghaile, P.Ó., Leech, D., and Magner, E. (2019). Use of polymer coatings to enhance the response of redox-polymer-mediated electrodes. *ChemElectroChem* 6, 1344–1349. <https://doi.org/10.1002/CELC.201800983>.
11. Bandodkar, A.J., You, J.M., Kim, N.H., Gu, Y., Kumar, R., Mohan, A.M.V., Kurniawan, J., Imani, S., Nakagawa, T., Parish, B., Parthasarathy, M., Mercier, P.P., Xu, S., and Wang, J. (2017). Soft, stretchable, high power density electronic skin-based biofuel cells for scavenging energy from human sweat. *Energy Environ. Sci.* 10, 1581–1589. <https://doi.org/10.1039/C7EE00865A>.
12. Szczupak, A., Halámek, J., Halámková, L., Bocharova, V., Alfonta, L., and Katz, E. (2012). Living battery – biofuel cells operating *in vivo* in clams. *Energy Environ. Sci.* 5, 8891–8895. <https://doi.org/10.1039/C2EE21626D>.
13. Zebda, A., Alcaraz, J.P., Vadgama, P., Shleev, S., Minteer, S.D., Boucher, F., Cinquin, P., and Martin, D.K. (2018). Challenges for successful implantation of biofuel cells. *Bioelectrochemistry* 124, 57–72. <https://doi.org/10.1016/j.bioelechem.2018.05.011>.
14. Tao, X. (2019). Study of fiber-based wearable energy systems. *Acc. Chem. Res.* 52, 307–315. <https://doi.org/10.1021/acs.accounts.8b00502>.
15. Chen, G., Li, Y., Bick, M., and Chen, J. (2020). Smart Textiles for Electricity Generation. *Chem. Rev.* 120, 3668–3720. <https://doi.org/10.1021/acs.chemrev.9b00821>.
16. Jeon, W.Y., Lee, J.H., Dashnyam, K., Choi, Y.B., Kim, T.H., Lee, H.H., Kim, H.W., and Kim, H.H. (2019). Performance of a glucose-reactive enzyme-based biofuel cell system for biomedical applications. *Sci. Rep.* 9, 10872. <https://doi.org/10.1038/s41598-019-47392-1>.
17. Bandodkar, A.J. (2017). Review—Wearable biofuel cells: Past, present and future. *J. Electrochem. Soc.* 164, H3007–H3014. <https://doi.org/10.1149/2.0031703JES>.
18. Buaki-Sogó, M., García-Carmona, L., Gil-Agustí, M., Zubizarreta, L., García-Pellicer, M., and Quijano-López, A. (2020). Enzymatic glucose-based bio-batteries: Bioenergy to fuel next-generation devices. *Top. Curr. Chem. (Cham)*. 378, 49. <https://doi.org/10.1007/S41061-020-00312-8>.
19. Zhang, J.L., Wang, Y.H., Huang, K., Huang, K.J., Jiang, H., and Wang, X.M. (2021). Enzyme-based biofuel cells for biosensors and *in vivo* power supply. *Nano Energy* 84, 105853. <https://doi.org/10.1016/J.NANOEN.2021.105853>.
20. Xiong, J., Chen, J., Lee, P.S., Xiong, J., Chen, J., and Lee, S. (2021). Functional fibers and fabrics for soft robotics, wearables, and human–robot interface. *Adv. Mater.* 33, 2002640. <https://doi.org/10.1002/ADMA.202002640>.
21. Xiao, X., Conghaile, P.Ó., Leech, D., Ludwig, R., and Magner, E. (2017). An oxygen-independent and membrane-less glucose biobattery/supercapacitor hybrid device. *Biosens. Bioelectron.* 98, 421–427. <https://doi.org/10.1016/J.BIOS.2017.07.023>.
22. Mano, N., and de Poulpique, A. (2018).  $\text{O}_2$  reduction in enzymatic biofuel cells. *Chem. Rev.* 118, 2392–2468. <https://doi.org/10.1021/acs.chemrev.7b00220>.
23. Tang, J., Werchmeister, R.M.L., Preda, L., Huang, W., Zheng, Z., Leimkühler, S., Wollenberger, U., Xiao, X., Engelbrekt, C., Ulstrup, J., and Zhang, J. (2019). Three-dimensional sulfite oxidase bioanodes based on graphene functionalized carbon paper for sulfite/ $\text{O}_2$  biofuel cells. *ACS Catal.* 9, 6543–6554. <https://doi.org/10.1021/ACSCATAL.9B01715>.
24. Werchmeister, R.M.L., Tang, J., Xiao, X., Wollenberger, U., Hjulter, H.A., Ulstrup, J., and Zhang, J. (2019). Three-dimensional bioelectrodes utilizing graphene based bioink. *J. Electrochem. Soc.* 166, G170–G177. <https://doi.org/10.1149/2.0261916JES>.
25. Feng, X., Xiao, X., Zhang, J., Guo, L., and Xiong, Y. (2021). Cobalt/nitrogen doped porous carbon as catalysts for efficient oxygen reduction reaction: Towards hybrid enzymatic biofuel cells. *Electrochim. Acta* 389, 138791. <https://doi.org/10.1016/J.ELECTACTA.2021.138791>.
26. Menassol, G., Dubois, L., Nadolska, M., Vadgama, P., Martin, D.K., and Zebda, A. (2023). A biocompatible iron doped graphene based cathode for an implantable glucose biofuel cell. *Electrochim. Acta* 439, 141627. <https://doi.org/10.1016/J.ELECTACTA.2022.141627>.
27. Santoro, C., Serov, A., Stariha, L., Kodali, M., Gordon, J., Babanova, S., Bretschger, O., Artyushkova, K., and Atanassov, P. (2016). Iron based catalysts from novel low-cost organic precursors for enhanced oxygen reduction reaction in neutral media microbial fuel cells. *Energy Environ. Sci.* 9, 2346–2353. <https://doi.org/10.1039/C6EE01145D>.
28. Xiao, X. (2022). The direct use of enzymatic biofuel cells as functional bioelectronics. *eScience* 2, 1–9. <https://doi.org/10.1016/j.esci.2021.12.005>.
29. Marcus, R.A. (1993). Electron transfer reactions in chemistry: Theory and experiment (Nobel Lecture). *Angew. Chem. Int. Ed. Engl.* 32, 1111–1121. <https://doi.org/10.1002/anie.199311113>.
30. Nazmutdinov, R.R., Shermokhamedov, S.A., Zinkicheva, T.T., Ulstrup, J., and Xiao, X. (2023). Understanding molecular and electrochemical charge transfer: theory and computations. *Chem. Soc. Rev.* 52, 6230–6253. <https://doi.org/10.1039/D2CS00006G>.
31. Chi, Q., Farver, O., and Ulstrup, J. (2005). Long-range protein electron transfer observed at the single-molecule level: *In situ* mapping of redox-gated tunneling resonance. *Proc. Natl. Acad. Sci. USA* 102, 16203–16208. <https://doi.org/10.1073/pnas.0508257102>.
32. Gutiérrez-Sánchez, C., Pita, M., Vaz-Domínguez, C., Shleev, S., and De Lacey, A.L. (2012). Gold nanoparticles as electronic bridges for laccase-based biocathodes. *J. Am. Chem. Soc.* 134, 17212–17220. <https://doi.org/10.1021/ja307308j>.
33. Page, C.C., Moser, C.C., Chen, X., and Dutton, P.L. (1999). Natural engineering principles of electron tunnelling in biological oxidation–reduction. *Nature* 402, 47–52. <https://doi.org/10.1038/46972>.
34. Katz, E., and Bollella, P. (2021). Fuel cells and biofuel cells: From past to perspectives. *Isr. J. Chem.* 61, 68–84. <https://doi.org/10.1002/IJCH.202000039>.
35. Tang, J., Yan, X., Huang, W., Engelbrekt, C., Duus, J.Ø., Ulstrup, J., Xiao, X., and Zhang, J. (2020). Bilirubin oxidase oriented on novel type three-dimensional biocathodes with reduced graphene aggregation for biocathode. *Biosens. Bioelectron.* 167, 112500. <https://doi.org/10.1016/J.BIOS.2020.112500>.
36. Yan, X., Tang, J., Tanner, D., Ulstrup, J., and Xiao, X. (2020). Direct electrochemical enzyme electron transfer on electrodes modified by self-assembled molecular monolayers. *Catalysts* 10, 1458. <https://doi.org/10.3390/catal10121458>.
37. Yan, X., Ma, S., Tang, J., Tanner, D., Ulstrup, J., Xiao, X., and Zhang, J. (2021). Direct electron transfer of fructose dehydrogenase immobilized on thiol-gold electrodes. *Electrochimica Acta* 392, 138946. <https://doi.org/10.1016/J.ELECTACTA.2021.138946>.
38. Yan, X., Tang, J., Ma, S., Tanner, D., Ludwig, R., Ulstrup, J., and Xiao, X. (2022). Engineering bio-interfaces for the direct electron transfer of *Myriococcus thermophilus* cellobiose dehydrogenase: Towards a mediator-less biosupercapacitor/biofuel cell hybrid. *Biosens. Bioelectron.* 210, 114337. <https://doi.org/10.1016/J.BIOS.2022.114337>.
39. Chaubey, A., and Malhotra, B.D. (2002). Mediated biosensors. *Biosens. Bioelectron.* 17, 441–456. [https://doi.org/10.1016/S0956-5663\(01\)00313-X](https://doi.org/10.1016/S0956-5663(01)00313-X).
40. Shen, F., Arshi, S., Magner, E., Ulstrup, J., and Xiao, X. (2022). One-step electrochemical approach of enzyme immobilization for bioelectrochemical applications. *Synth. Met.* 291, 117205. <https://doi.org/10.1016/J.SYNTHMET.2022.117205>.
41. Xiao, X., Yan, X., Magner, E., and Ulstrup, J. (2021). Polymer coating for improved redox-polymer-mediated enzyme electrodes: A mini-review. *Electrochem. Commun.* 124, 106931. <https://doi.org/10.1016/J.ELECOM.2021.106931>.
42. Yuan, M., and Minteer, S.D. (2019). Redox polymers in electrochemical systems: From methods of mediation to energy storage. *Curr. Opin. Electrochem.* 15, 1–6. <https://doi.org/10.1016/J.COELEC.2019.03.003>.
43. Xiao, X., Xia, H.Q., Wu, R., Bai, L., Yan, L., Magner, E., Cosnier, S., Lojou, E., Zhu, Z., and Liu, A. (2019). Tackling the challenges of enzymatic (bio)fuel cells. *Chem. Rev.* 119, 9509–9558. <https://doi.org/10.1021/ACS.CHEMREV.9B00115>.
44. Shen, F., Cao, X., Pankratov, D., Zhang, J., and Chi, Q. (2017). Nanoengineering of graphene-supported functional composites for performance-enhanced enzymatic biofuel

- cells. In *Graphene Bioelectronics* (Elsevier Inc), pp. 219–240. <https://doi.org/10.1016/B978-0-12-813349-1.00010-X>.
45. Xiao, X., Wang, M., Li, H., and Si, P. (2013). One-step fabrication of bio-functionalized nanoporous gold / poly (3,4-ethylenedioxythiophene) hybrid electrodes for amperometric glucose sensing. *Talanta* 116, 1054–1059. <https://doi.org/10.1016/j.talanta.2013.08.014>.
  46. Xiao, X., Conghaile, P.Ó., Leech, D., Ludwig, R., and Magner, E. (2017). A symmetric supercapacitor/biofuel cell hybrid device based on enzyme-modified nanoporous gold: An autonomous pulse generator. *Biosens. Bioelectron.* 90, 96–102. <https://doi.org/10.1016/j.bios.2016.11.012>.
  47. Xiao, X., Siepenkoetter, T., Whelan, R., Salaj-Kosla, U., and Magner, E. (2018). A continuous fluidic bioreactor utilising electrodeposited silica for lipase immobilisation onto nanoporous gold. *J. Electroanal. Chem.* 812, 180–185. <https://doi.org/10.1016/j.jelechem.2017.11.059>.
  48. Gamella, M., Koushanpour, A., and Katz, E. (2018). Biofuel cells – Activation of micro- and macro-electronic devices. *Bioelectrochemistry* 119, 33–42. <https://doi.org/10.1016/j.bioelechem.2017.09.002>.
  49. Wang, L., He, E., Gao, R., Wu, X., Zhou, A., Lu, J., Zhao, T., Li, J., Yun, Y., Li, L., Ye, T., Jiao, Y., Wang, J., Chen, H., Li, D., Ning, X., Wu, D., Peng, H., and Zhang, Y. (2021). Designing porous antifouling interfaces for high-power implantable biofuel cell. *Adv. Funct. Mater.* 31, 2107160. <https://doi.org/10.1002/adfm.202107160>.
  50. Wu, J.-G., Chen, J.-H., Liu, K.-T., and Luo, S.-C. (2019). Engineering antifouling conducting polymers for modern biomedical applications. *ACS Appl. Mater. Interfaces* 11, 21294–21307. <https://doi.org/10.1021/acsami.9b04924>.
  51. Kwon, C.H., Ko, Y., Shin, D., Kwon, M., Park, J., Bae, W.K., Lee, S.W., and Cho, J. (2018). High-power hybrid biofuel cells using layer-by-layer assembled glucose oxidase-coated metallic cotton fibers. *Nat. Commun.* 9, 4479. <https://doi.org/10.1038/s41467-018-06994-5>.
  52. Guo, Y., Chen, C., Feng, J., Wang, L., Wang, J., Tang, C., Sun, X., and Peng, H. (2022). An anti-biofouling flexible fiber biofuel cell working in the brain. *Small Methods* 6, e2200142. <https://doi.org/10.1002/smdt.202200142>.
  53. Mano, N., Mao, F., and Heller, A. (2002). A miniature biofuel cell operating in a physiological buffer. *J. Am. Chem. Soc.* 124, 12962–12963. <https://doi.org/10.1021/ja028514g>.
  54. Yin, S., Liu, X., Kobayashi, Y., Nishina, Y., Nakagawa, R., Yanai, R., Kimura, K., and Miyake, T. (2020). A needle-type biofuel cell using enzyme/mediator/carbon nanotube composite fibers for wearable electronics. *Biosens. Bioelectron.* 165, 112287. <https://doi.org/10.1016/j.bios.2020.112287>.
  55. Sim, H.J., Lee, D.Y., Kim, H., Choi, Y.B., Kim, H.H., Baughman, R.H., and Kim, S.J. (2018). Stretchable fiber biofuel cell by rewinding multiwalled carbon nanotube sheets. *Nano Lett.* 18, 5272–5278. <https://doi.org/10.1021/acs.nanolett.8b02256>.
  56. Wang, L., Xie, S., Wang, Z., Liu, F., Yang, Y., Tang, C., Wu, X., Liu, P., Li, Y., Saiyin, H., Zheng, S., Sun, X., Xu, F., Yu, H., and Peng, H. (2020). Functionalized helical fibre bundles of carbon nanotubes as electrochemical sensors for long-term *in vivo* monitoring of multiple disease biomarkers. *Nat. Biomed. Eng.* 4, 159–171. <https://doi.org/10.1038/s41551-019-0462-8>.
  57. Chen, S., Li, L., Zhao, C., and Zheng, J. (2010). Surface hydration: Principles and applications toward low-fouling/nonfouling biomaterials. *Polymer* 51, 5283–5293. <https://doi.org/10.1016/J.POLYMER.2010.08.022>.
  58. Rabinow, B.E., Ding, Y.S., Qin, C., McHalsky, M.L., Schneider, J.H., Ashline, K.A., Shelbourn, T.L., and Albrecht, R.M. (1994). Biomaterials with permanent hydrophilic surfaces and low protein adsorption properties. *J. Biomater. Sci. Polym. Ed.* 6, 91–109. <https://doi.org/10.1163/156856295X00788>.
  59. Wei, Q., Becherer, T., Angioletti-Uberti, S., Dzubiella, J., Wischke, C., Neffe, A.T., Lendlein, A., Ballauff, M., and Haag, R. (2014). Protein interactions with polymer coatings and biomaterials. *Angew. Chem. Int. Ed. Engl.* 53, 8004–8031. <https://doi.org/10.1002/ANIE.201400546>.
  60. Qian, Z., Yang, Y., Wang, L., Wang, J., Guo, Y., Liu, Z., Li, J., Zhang, H., Sun, X., and Peng, H. (2023). An implantable fiber biosupercapacitor with high power density by multi-strand twisting functionalized fibers. *Angew. Chem. Int. Ed. Engl.* 62, e202303268. <https://doi.org/10.1002/ANIE.202303268>.
  61. Xiao, G., Ju, J., Li, M., Wu, H., Jian, Y., Sun, W., Wang, W., Li, C.M., Qiao, Y., and Lu, Z. (2023). Weavable yarn-shaped supercapacitor in sweat-activated self-charging power textile for wireless sweat biosensing. *Biosens. Bioelectron.* 235, 115389. <https://doi.org/10.1016/J.BIOS.2023.115389>.
  62. Kwon, C.H., Lee, S.-H., Choi, Y.-B., Lee, J.A., Kim, S.H., Kim, H.-H., Spinks, G.M., Wallace, G.G., Lima, M.D., Kozlov, M.E., Baughman, R.H., and Kim, S.J. (2014). High-power biofuel cell textiles from woven bisrolled carbon nanotube yarns. *Nat. Commun.* 5, 3928. <https://doi.org/10.1038/ncomms4928>.
  63. Kwon, C.H., Lee, J.A., Choi, Y.B., Kim, H.H., Spinks, G.M., Lima, M.D., Baughman, R.H., and Kim, S.J. (2015). Stability of carbon nanotube yarn biofuel cell in human body fluid. *J. Power Sources* 286, 103–108. <https://doi.org/10.1016/j.jpowsour.2015.03.140>.
  64. Latonen, R.-M., Akie, M.N., Vavra, K., Bobacka, J., and Ivaska, A. (2013). Ion exchange behavior of polypyrrole doped with large anions in electrolytes containing mono- and divalent metal ions. *Electroanalysis* 25, 991–1004. <https://doi.org/10.1002/elan.201200566>.
  65. Tóth, P.S., Janáky, C., Berkesi, O., Tamm, T., and Visy, C. (2012). On the unexpected cation exchange behavior, caused by covalent bond formation between PEDOT and Cl<sup>-</sup> ions: Extending the conception for the polymer-dopant interactions. *J. Phys. Chem. B* 116, 5491–5500. <https://doi.org/10.1021/JP2107268>.
  66. Elad, D., and Einav, S. (2004). Physical and flow properties of blood. In *Standard handbook of biomedical engineering and design*, K. Myer, ed. (McGraw-Hill). [www.digitalengineeringlibrary.com](http://www.digitalengineeringlibrary.com).
  67. Lee, D.Y., Yun, J.H., Park, Y.B., Hyeon, J.S., Jang, Y., Choi, Y.B., Kim, H.H., Kang, T.M., Ovalle, R., Baughman, R.H., Kim, S.M., Kee, C.W., and Kim, S.J. (2020). Two-ply carbon nanotube fiber-typed enzymatic biofuel cell implanted in mice. *IEEE Trans. NanoBioscience* 19, 333–338. <https://doi.org/10.1109/TNB.2020.2995143>.
  68. Kwon, C.H., Park, Y.B., Lee, J.A., Choi, Y.B., Kim, H.H., Lima, M.D., Baughman, R.H., and Kim, S.J. (2016). Mediator-free carbon nanotube yarn biofuel cell. *RSC Adv.* 6, 48346–48350. <https://doi.org/10.1039/c6ra06570h>.
  69. Jeeran, I., Sempionatto, J.R., Pavinatto, A., You, J.M., and Wang, J. (2016). Stretchable biofuel cells as wearable textile-based self-powered sensors. *J. Mater. Chem. A Mater.* 4, 18342–18353. <https://doi.org/10.1039/C6TA08358G>.
  70. Lv, J., Jeeran, I., Tehrani, F., Yin, L., Silva-Lopez, C.A., Jang, J.H., Joshua, D., Shah, R., Liang, Y., Xie, L., Soto, F., Chen, C., Karshalev, E., Kong, C., Yang, Z., and Wang, J. (2018). Sweat-based wearable energy harvesting-storage hybrid textile devices. *Energy Environ. Sci.* 11, 3431–3442. <https://doi.org/10.1039/c8ee02792g>.
  71. Yin, L., Kim, K.N., Lv, J., Tehrani, F., Lin, M., Lin, Z., Moon, J.M., Ma, J., Yu, J., Xu, S., and Wang, J. (2021). A self-sustainable wearable multi-modular E-textile bioenergy microgrid system. *Nat. Commun.* 12, 1542. <https://doi.org/10.1038/s41467-021-21701-7>.
  72. Kai, H., Kato, Y., Toyosato, R., and Nishizawa, M. (2018). Fluid-permeable enzymatic lactate sensors for micro-volume specimen. *Analyst* 143, 5545–5551. <https://doi.org/10.1039/c8an00979a>.
  73. Chen, Z., Yao, Y., Lv, T., Yang, Y., Liu, Y., and Chen, T. (2022). Flexible and stretchable enzymatic biofuel cell with high performance enabled by textile electrodes and polymer hydrogel electrolyte. *Nano Lett.* 22, 196–202. <https://doi.org/10.1021/acs.nanolett.1c03621>.
  74. Yin, S., Jin, Z., and Miyake, T. (2019). Wearable high-powered biofuel cells using enzyme/carbon nanotube composite fibers on textile cloth. *Biosens. Bioelectron.* 141, 111471. <https://doi.org/10.1016/j.bios.2019.111471>.